Investigating the Inhibition of Mild Steel Corrosion by *Tectona grandis* dye Extracts in Acidic Environments: Thermodynamics and Adsorption Properties Characterization

ABSTRACT

An investigation into the corrosion inhibition potential of Tectona grandis dye extract on mild steel in 1 M HCl was conducted using weight loss and electrochemical techniques. Adsorption and thermodynamic parameters were also evaluated to understand the influence of extract structure on inhibition performance. Analysis revealed that Tectona grandis dye extract exhibited light absorption adsorption properties characteristic of a dye molecule, the Phytochemical analysis of Tectona grandis dye extract shows the presence of Alkaloids, flavonoids, saponins phenols, anthraquinones, and tannins, the result also demonstrated a direct correlation between extract concentration and inhibition efficiency, while an inverse correlation was observed with temperature. Increased activation energy in inhibited solutions supported the temperature dependence. Positive ΔH^0 ΔH^o values indicated an endothermic reaction, and negative ΔG^0_{ads} $\Delta G^o_{ads.}$ values suggested spontaneous adsorption following the Langmuir and Freundlich isotherm models. Potentiodynamic polarization curves revealed mixed-type inhibition behavior. These findings suggest the Tectona grandis dye extract possesses promising corrosion inhibition properties.

KEY WORDS: *Corrosion, Mild Steel, Hydrochloric Acid, Corrosion Rate, Tectona grandis*

I- INTRODUCTION

Preventing Prevention of metal rust and decay (corrosion) is a constant battle in many industries and scientific fields**.** The most common weapon in this fight is Corrosion inhibitors. These act like a protective shield on metal surfaces, clinging tightly and blocking out harmful chemicals that can cause damage. Research has shown that specific molecules containing nitrogen, oxygen, or sulfur atoms, particularly those arranged in ring or chain-like structures, are particularly effective at inhibiting corrosion [1]. Plant extracts are gaining ground as a promising alternative for corrosion inhibitors. These natural solutions have shown effectiveness in preventing metal from rusting and degrading.[2-4].Studies on the chemical composition of teak (Tectona grandis) have identified interesting groups of molecules that might act as corrosion inhibitors. These

include tannins, alkaloids, flavonoids, anthraquinones, and naphthoquinones. Notably, these molecules contain oxygen (O) and nitrogen (N) atoms, which are often linked to corrosion inhibition properties, along with functional groups that could potentially hinder corrosion processes. [5]. While previous research has explored Tectona grandis leaf extract as a corrosion inhibitor for mild steel in acidic environments [6-8], the specific effectiveness of Tectona grandis dye extract in this role remains scanty.

II- MATERIALS AND METHODS

Extraction of Tectona grandis Dye (TG dye)

The teak (*Tectona grandis*) leaves for dye extraction were meticulously cleaned to remove any dirts. Once clean, the leaves were carefully dried in the shade for three weeks to ensure they were completely free of moisture. After drying, the leaves were crushed into a fine powder using a grinder. Sifting the powder ensured a consistent particle size for optimal dye extraction. Five hundred grams of the powdered leaves were submerged in two liters of a 50% ethanol solution and soaked for three days. This allows the solvent (ethanol) to dissolve the dye compounds from the leaves. After soaking, the mixture was filtered to separate the concentrated dye extract (a liquid) from the solid leftover leaf material. Finally, the extract was further concentrated, using a rotary evaporator, and stored in a refrigerator for later use.

Phytochemical analysis

A well-documented techniques was were used to identify the chemical components within the TG dye extract [9-11].

UV-Visible spectrophotometer

The absorbance of the TG dye extract was measured between 200 and 800 nanometers using a Genesys 10S UV-Visible spectrophotometer.

Fourier transform infrared (FTIR) spectroscopy

The chemical functionality of the TG dye extract was analyzed using an Agilent Technologies FTIR spectrophotometer across a wide range, from 600 to 4000 cm^{-1} cm^{-1}.

Corrosion inhibition studies …may be this title cancel and shift the following part before UV visible spectrophotometer and after phytochemical analysis

Preparation of mild steel Composition of mild steel

The mild steel consisted primarily of iron (Fe) with small amounts of manganese (Mn), carbon (C), chromium (Cr), sulfur (S), and nickel (Ni).

Corrosive and inhibitor environments Preparation ***Corrosive environment and inhibitor preparation***

A 1.0 M hydrochloric acid (HCl) solution was prepared and Inhibitor solutions with concentrations ranging from 0.2 to 1.2 grams per liter (g/L)(g/l) were created by dissolving precisely weighed quantities of the plant extract and silver nanoparticles in the 1.0 M HCl solution.

Shift the previous part

Weight-loss measurements

The already weighed coupons were immersed in the HCl solution for 3 hours at 303 K, both with and without the presence of varying concentrations of *Tectona grandis* (TG) crude extract and nanoparticles. Once submerged, the metal samples were taken out, washed in a special solution (NaOH), rinsed with clean water and acetone, dried completely, and then weighed again to see how much metal was lost. Each experiment was performed trice to ensure data accuracy. The average weight loss values were then used for the calculation using Equations (1), (2), and (3) as described in [11].

$$C.R = \frac{\Delta w}{At} \qquad\qquad (1)$$

Where Δw = change in weight in g

A = Area in cm^2

t = Time in hour

% I.E = I - $\frac{\Delta w_1}{\Delta w_2}$ x 100   …   % I.E = 1 – $\qquad\qquad$ (2)

Where where Δw_1 and Δw_2 are uninhibited and inhibited weight loss measurements.

$\Theta = 1 - \frac{\Delta w_1}{\Delta w_2}$ $\qquad\qquad$ (3)

The procedure was repeated at temperature values of 313K, 323K, and 323K.

Electrochemical Studies

The corrosion resistance of the mild steel was evaluated using a three-electrode setup connected to an electrochemical workstation. This setup included a platinum counter electrode, a saturated calomel electrode (SCE) as a reference point, electrode and the mild steel itself as the working electrode. To **assess its** corrosion behavior, the working electrode was scanned across a range of voltages. The voltage started -250 millivolts (mV) negative (cathodic) and increased to ±250 mV positive (anodic) relative to the initial open circuit potential (OCP) of the system. This scan was done at a slow and steady rate of 1 mV per second, generating a plot of current versus voltage (potentiodynamic curve). It's important to note that all voltage measurements were referenced to the SCE for consistency. Interestingly, the same piece of mild steel was used for both the following tests without any additional cleaning in between. The first test, called electrochemical impedance spectroscopy (EIS), involved applying a tiny alternating voltage (10 mV) at various frequencies (20 kHz to 200 Hz). This helps us understand how the steel responds to small electrical disturbances, which can be related to corrosion processes. Corrosion inhibition efficiency (IE%) was calculated based on the analysis of the polarization plots using the following equation.

$$IE\% = 1 - \left(\frac{i_{corr}}{i_{corr}^{o}} \right) \times 100\% \qquad (4)$$

Based on the measurements, a graphs (Nyquist and Bode plots) was were obtained that can be used to calculate percent efficiency (IE%) , which indicates how effective the corrosion inhibitor. is

% IE =

$$IE = \left(\frac{R_{ct} - R_{ct}^{\circ}}{R_{ct}} \right) \times 100\%, \qquad (5)$$

where R_{ct} and R_{ct}^{o} represent charge transfer resistance in the with and without inhibitor concentrations.

Analysis of a surface's shape and features

The surface characteristics of mild steel coupons after exposure to 1.0 M HCl solutions Was were investigated using scanning electron microscopy (SEM). The SEM analysis was performed in a vacuum environment at 15 kV on both untreated samples and those immersed in solutions with varying concentrations of Tectona grandis (TG) dye. Additionally, energy-dispersive X-ray spectroscopy analysis (EDX) was employed to analyze the elemental composition of the coupon surfaces.

III- RESULTS AND DISCUSSION

Investigation of the phytochemical profile

Phytochemical analysis of TG dye extract shows the presence of Alkaloids, flavonoids, saponins phenols, anthraquinones, and tannins. Previous investigators showed that saponins, tannins, and alkaloids are the active constituents of some of the green inhibitors [5].

Table 1: Investigation of the phytochemical profile of TG dye extract

Parameter	Observation
Alkaloids	+++
Flavonoids	++
Saponins	++
Cardiac Glycosides	++
Anthraquinones	++
Tannins	++
Phenols	+++

UV-Visible spectrophotometer

The TG dye extract reveals its chemical structure through its unique light absorption pattern. The UV-vis spectrum shows two distinct peaks at 241.4 nm and 376 nm. These peaks are characteristic of aromatic molecules, which are common in dye molecules. Interestingly, this pattern is similar to what's observed in certain flavonoid compounds [12]. Flavonoids, a class of natural pigments, are known for their aromatic structures that absorb light around 250 nm, as confirmed by previous research [12]. This absorption likely corresponds to the energy boost of

electrons within the molecule. Additionally, the presence of carbonyl groups (another common structural feature in flavonoids) can contribute to further light absorption around 300 nm [12]. Even more intriguing, the peaks we observed closely match the light absorption profile of quercetin, a specific type of flavonoid. This suggests that quercetin might be a significant component of the TG dye extract, as it's known to absorb light across a wide range (240-500 nm) in the UV-visible spectrum.[13][17].[13-17].
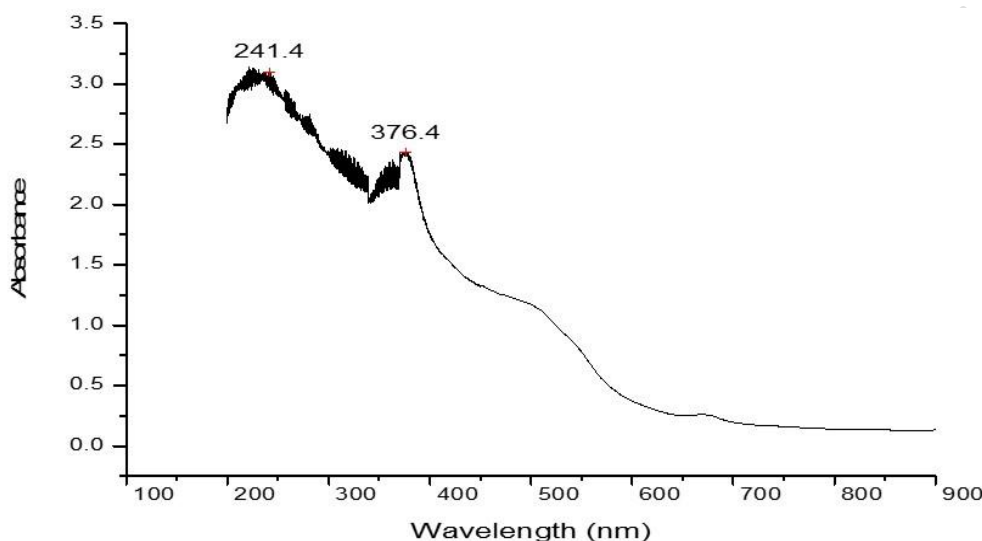

Fig. 1: UV–Vis absorption spectrum of **TG dye**

FT-IR Analysis

The FT-IR spectrum of the TG dye extract (Figure 2) reveals the presence of various functional groups with characteristic absorption bands ranging from 3294.96 cm-1 cm^{-1}to 812.56 cm^{-1}. The broad band observed between 3294.96 cm^{-1} and 3268.97 cm^{-1} can be attributed to either C-H stretching vibrations in amines or O-H stretching vibrations in alcohols [14]. The peaks between 2929.6 cm^{-1} and 2855.14 cm-1 correspond to C-H bending vibrations, while the band between 1733.21 cm^{-1} and 1625.11 cm^{-1} indicates the presence of C=C or C=O stretching vibrations [15, 16]. These observations suggest that the TG dye extract contains functional groups with O-H, C=O, C=C, and C-H functionalities, which are commonly associated with effective corrosion

inhibitors.
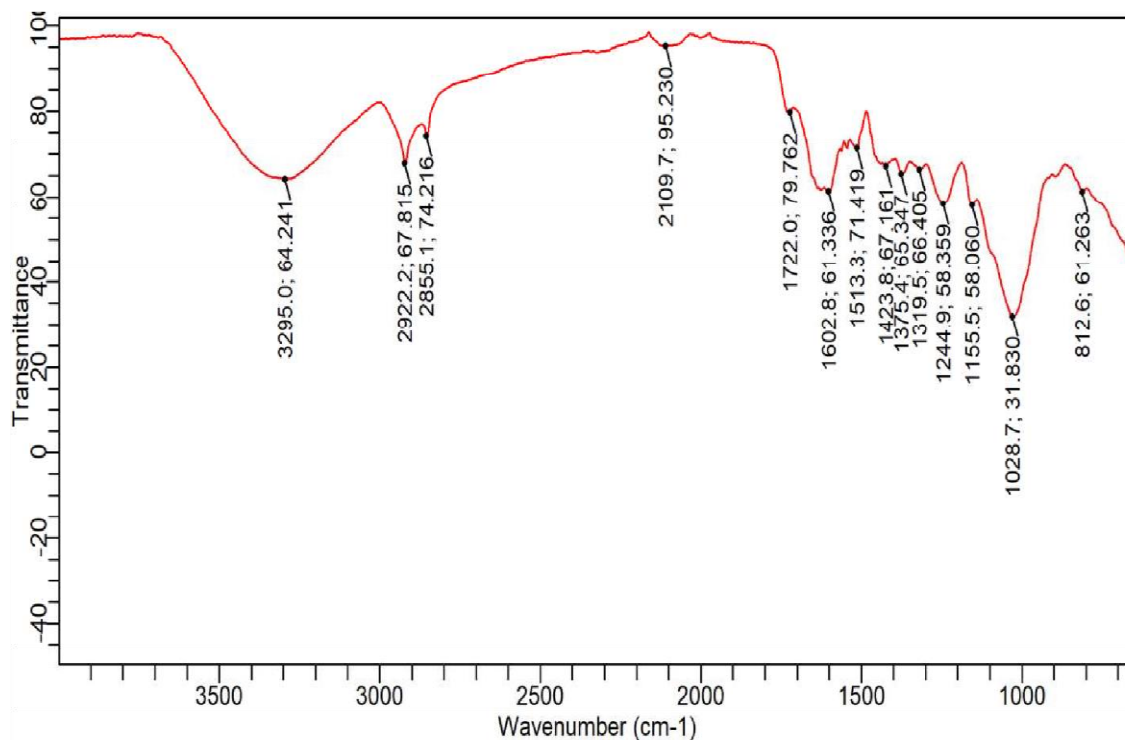
Fig. 2: **FTIR spectrum of TG dye**

Corrosion inhibitory studies…Effect of corrosion inhibitor on corrosion rate
The weight loss measurements
Corrosion Rates … this title may be cancel….

Figures 3 show how the Tectona grandis dye extract (TG) impacts in reduce corrosion rates. The data reveals that corrosion rates increase as the temperature rises. This likely happens because the protective layer formed by the TG dye degrades at higher temperatures. Additionally, hotter environments accelerate the production of hydrogen gas, which can further worsen corrosion [17]. Conversely, the corrosion rate decreases as the concentration of the TG dye extract increases. This significant reduction highlights the effectiveness of the TG dye in slowing down corrosion.
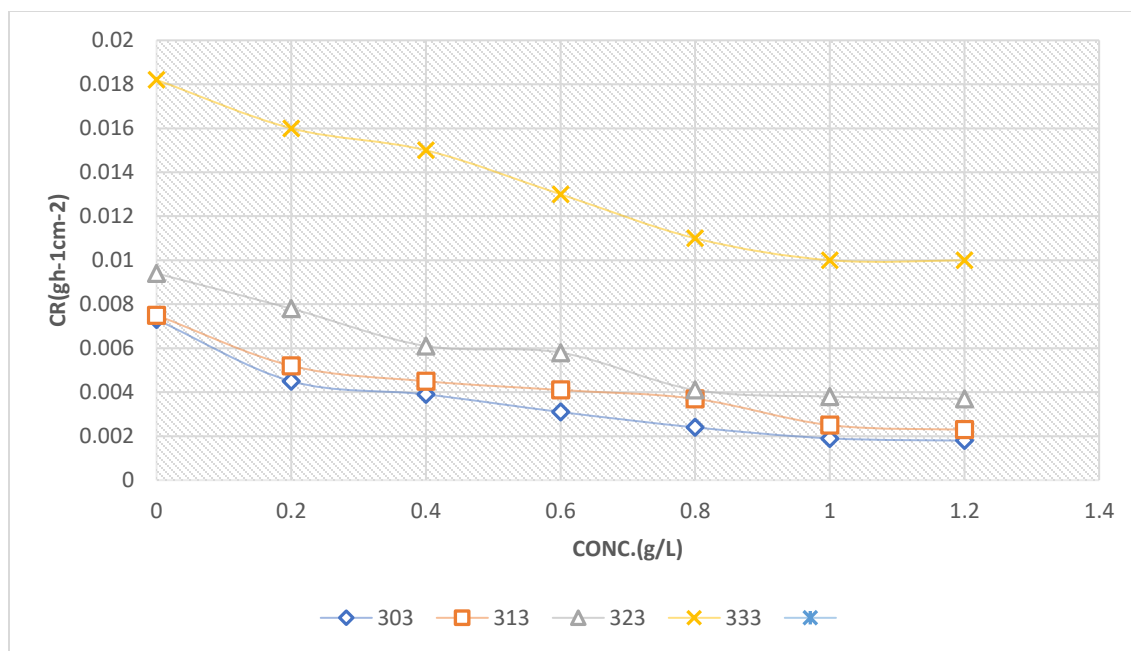
Fig.3: Corrosion Rate in presence and absence of TG dye ..<u>Effect of TG dye on corrosion rate</u>

<u>*Effect of TG dye on* I</u>*nhibition efficiency* <u>*percentage*</u>

Figure 4 shows how well the Tectona grandis (TG) dye extract inhibits corrosion., <u>using a measurement called 'percentage inhibition efficiency' (IE).</u> The higher <u>the</u> <u>%</u> IE, the better the protection. the <u>%</u> IE increases as we add more TG dye. This is consistent with what other researchers have found [18]. It suggests that using even higher concentrations of TG dye could provide even greater protection against corrosion. The success of the TG dye extract as a corrosion inhibitor likely hinges on the presence of specific natural ingredients. These include tannins, flavonoids, polyphenols, and alkaloids. These molecules act like tiny shields because they contain atoms like nitrogen, sulfur, and oxygen that can bond with the iron atoms on the metal surface. This creates a protective layer, like a shield, called a "passivation layer," that prevents corrosive ions from reaching and damaging the metal. The changes observed in certain peaks of the FT-IR analysis further support this idea of a barrier forming between the inhibitor and the steel surface. It's worth noting that many studies have shown the effectiveness of natural plant extracts like this one in preventing corrosion [19].
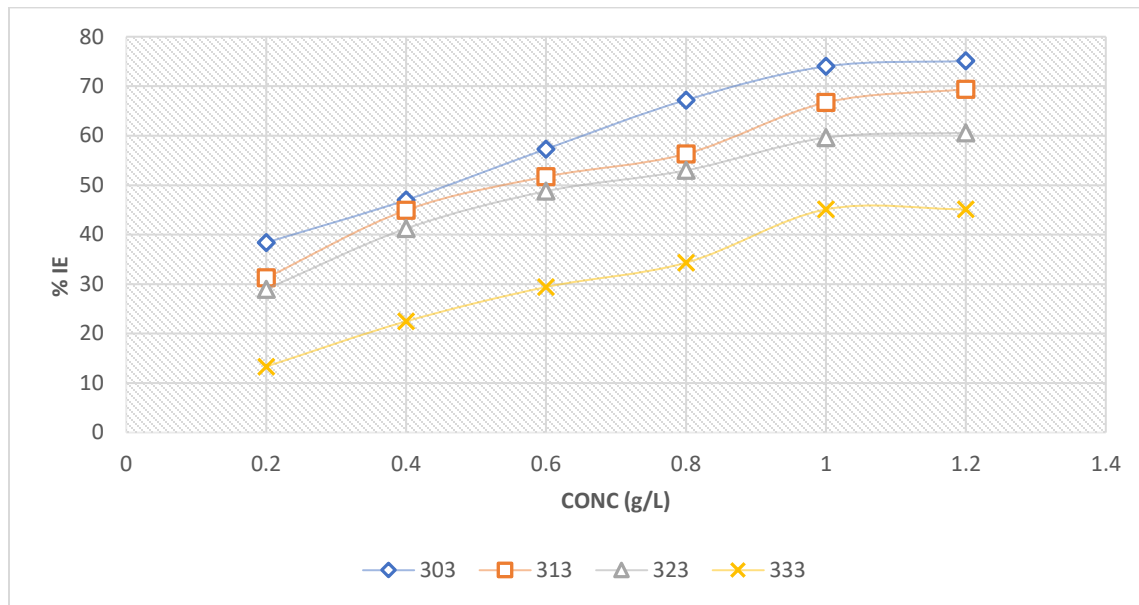
**Fig.4:** *Effect of TG dye on Inhibition efficiency of TG dye*

Electrochemical studies

Potentiodynamic polarization measurements

Tafel polarization curves (Figure 5) reveal several key corrosion parameters, including cathodic and anodic Tafel slopes (β_c and β_a), corrosion potential ($E_{corr.}$), and corrosion current ($I_{corr.}$) (Table 2). Interestingly, the consistent linearity of the cathodic curves despite increasing dye extract concentration implies that the extract doesn't fundamentally change the mechanism of hydrogen gas evolution during corrosion."

However, a significant change in the cathodic Tafel slope (β_c) values is observed (Table 2), implying that the dye extract significantly influences the kinetics of hydrogen gas evolution on the mild steel surface [20]. This translates to a notable decrease in the measured corrosion current ($I_{corr.}$) for inhibited solutions compared to the uninhibited one.

Furthermore, the maximum deviation in corrosion potential ($E_{corr.}$) values across all inhibitor concentrations remains less than 85 mV (Table 2). Based on this observation, the inhibitor can be classified as a mixed-type inhibitor according to established criteria [20]. This classification

indicates that the inhibitor likely affects both the cathodic and anodic reactions responsible for the corrosion process.
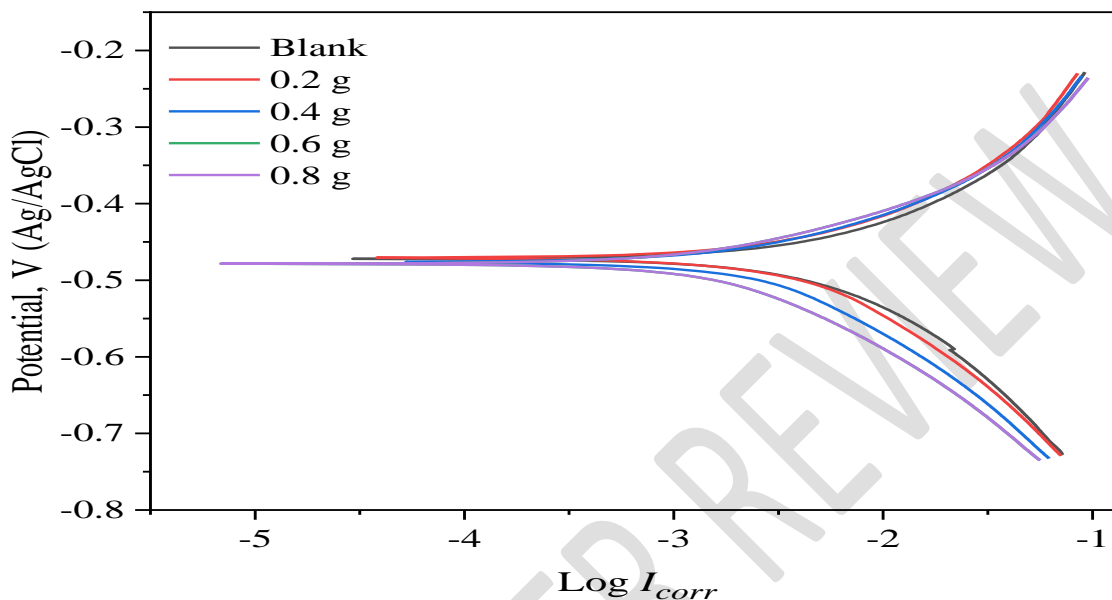
Fig.5: Potentiodynamic polarization curves for mild steel in various concentration with and without (TG) dye.

xxxx Note: Fig. 5 present on y-axis potential (Ag/AgCl), that may be correct to potential (SCE)

Table 2: Potentiodynamic polarization characteristics for mild steel in various concentration with and without (TG) dye.

Concentration ($g\ L^{-1}$)(gl^{-1})	$-E_{corr.}$ (mV)	$i_{corr.}$ (mA cm^{-2})	β_a (mV dec^{-1})	$-\beta_c$ (mV dec^{-1})	IE (%)
blank	472.05	108.05	151.87	216.2	-
TG					
0.2	465.49	87.03	104.42	170.05	19.45
0.4	470.78	70.18	102.49	154.95	35.05
0.6	472.53	64.29	73.904	136.9	40.50
0.8	475.23	49.3	87.825	152.05	54.37

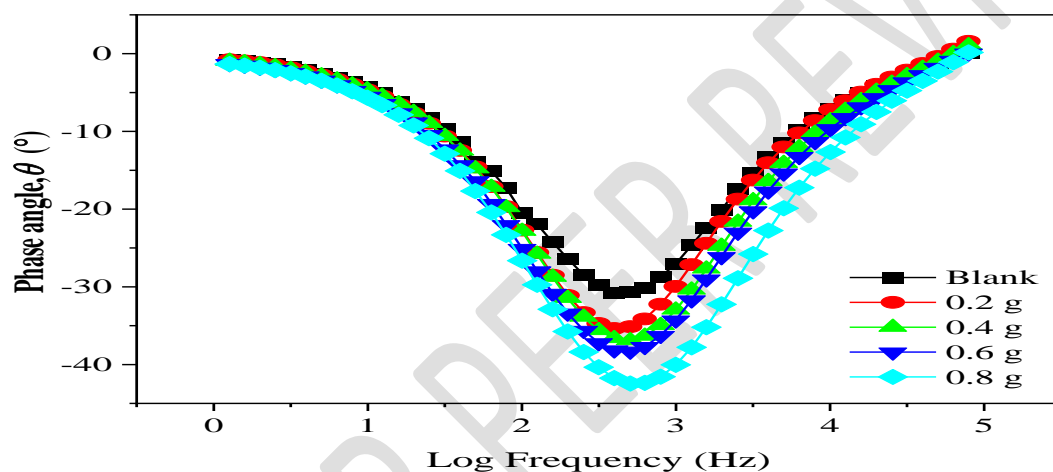***Electrochemical Impedance Spectroscopy (EIS) measurements***

Electrochemical Impedance Spectroscopy (EIS) measurements, provided a deeper understanding of how the inhibitor works (mechanism) to prevent corrosion. A specific plot type, the Nyquist plot (Figure 6), showed incomplete circles, indicating a combination of two processes at the metal's surface where it meets the electrolyte: resistance to electron transfer and resistance within small pores. Additional figures (Bode plots) (Figures 7a and 7b) offer more details about the electrical properties of the system. Key parameters obtained from the EIS data are summarized in Table 3.The Nyquist plots (Figure 6) clearly show a trend. As the inhibitor concentration increases, the size of the semicircles gets bigger. This indicates a rise in a value called "charge transfer resistance" (R_{ct}), which is a key measure of how effective the inhibitor is. Higher R_{ct} values mean the inhibitor molecules create a stronger barrier on the metal surface, significantly slowing down corrosion. Adding the inhibitor also lowers the capacitance of the double layer (C_{dl}). This is likely because the inhibitor creates a thicker layer on the metal surface, as seen in other research [20].
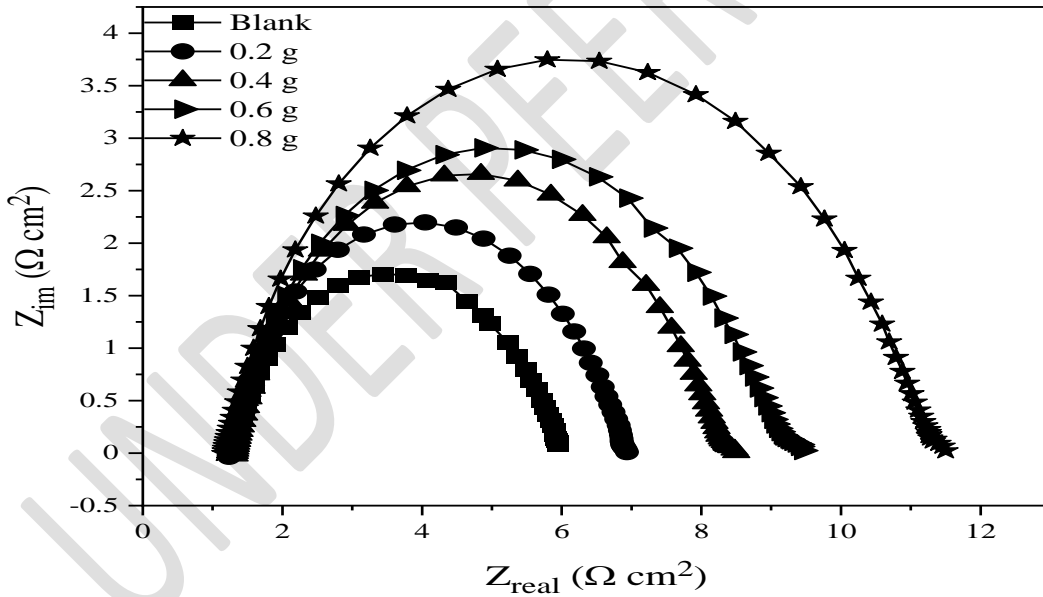
Fig. 6: Nyquist plots for mild steel corrosion in 1M HCl with and without (TG) dye
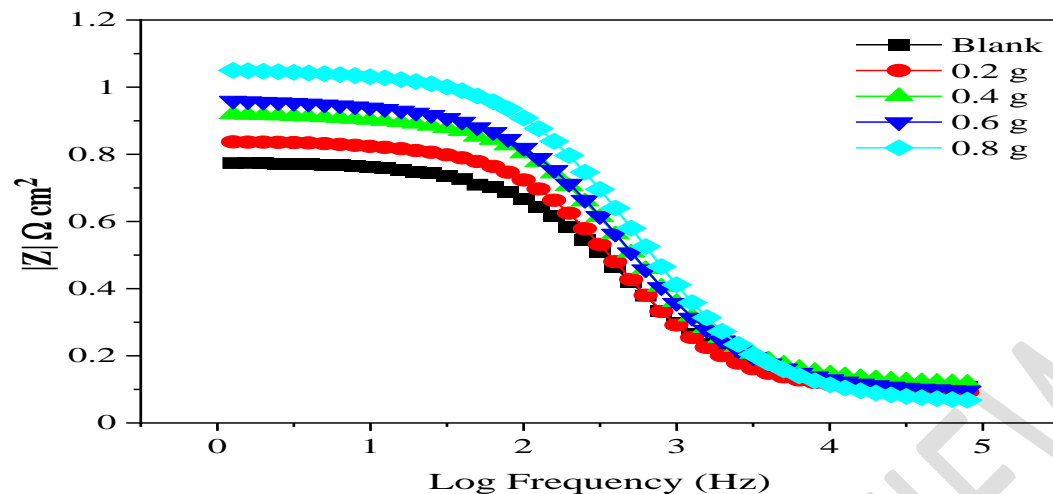
(a)

(b)

Fig.7(a) and (b): Bode plots for mild steel corrosion in 1M HCl with and without (TG) dye
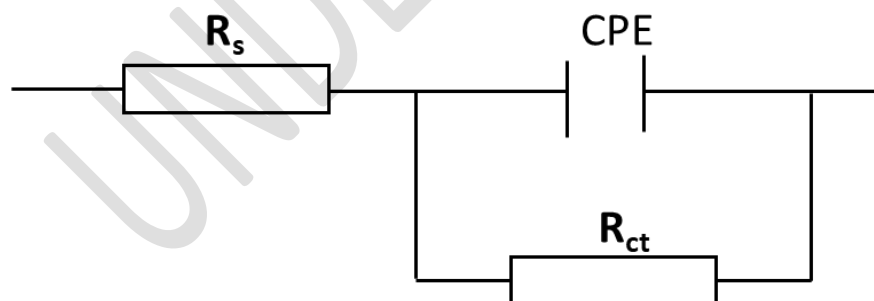

Fig. 8: Randle circuit for fitting the EIS data...The equivalent circuit diagram

Table 3: Electrochemical Impedance Spectroscopy characteristics of mild steel in 1M HCl with and without (TG) dye

Concentration (g L⁻¹)	R_s (Ω cm²)	R_{ct} (Ω cm²)	Y_o (x 10⁻³ sⁿ Ω^{-1} cm⁻²)	n	C_{dl} (x 10⁶ F cm²)	IE (%)
Blank	2.7458	1.8236	9.202	1.5843	9.8163	-
TG						
0.2	2.948	2.2195	7.4637	1.5814	7.6649	17.84
0.4	3.4312	2.7204	6.0682	1.5803	6.1426	32.97
0.6	3.5524	3.1367	5.7823	1.5771	5.6125	41.86
0.8	4.1231	4.0347	4.4813	1.5787	4.4420	54.80

Thermodynamics and Adsorption Isotherms Evaluation

**Effect of Inhibitor on Activation Energy and Thermodynamic Parameters**

The Arrhenius equation and the slopes of the log CR vs 1/T plots was were used to calculate the activation energy (E_a). As the Table (3) shows, the E_a values for the acid solution with the inhibitor are significantly higher than those without the inhibitor (Table 3).

This observation suggests that the presence of the inhibitor increases the energy barrier required for the corrosion reaction to occur, supporting the physical adsorption mechanism.

The plot of log CR/T versus 1/T for mild steel in 1 M HCl solution with and without varying inhibitor concentrations resulted in a straight line (Arrhenius plot). The intercept and slope of this line correspond to the equation:

$$\log (R/Nh) + \Delta S^o_{ads} / 2.303R \Delta H^o_{ads} / 2.303R \qquad \text{xxx this equation not correct and no present (=)} \qquad (4)…(6)$$

R (the gas constant), Nh (Planck's constant), ΔS^o_{ads} (entropy of adsorption), and ΔH^o_{ads} (enthalpy of adsorption). Table 4 shows the values of ΔH^o_{ads} and ΔS^o_{ads}, calculated from the slope and intercept of the plot. The positive value of ΔH^o_{ads} suggests the steel dissolution process is endothermic. This means the reaction absorbs heat from its surroundings to proceed
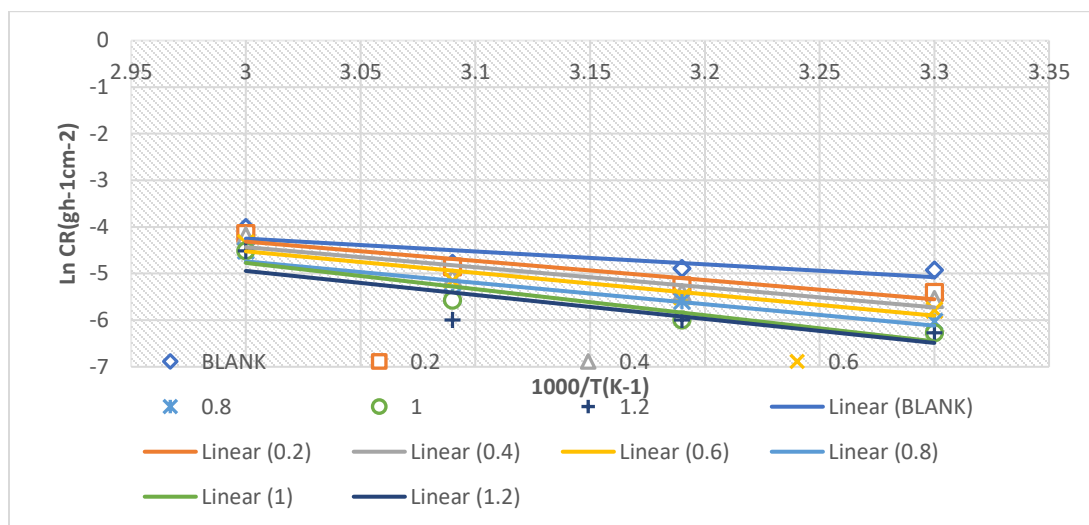
Fig. 9: *Arrhenius plots for different concentrations of* TG Dye *and blank* *..Relationship between ln CR and 1/T* for mild steel in 1 M HCl solution in different concentration of TG dye
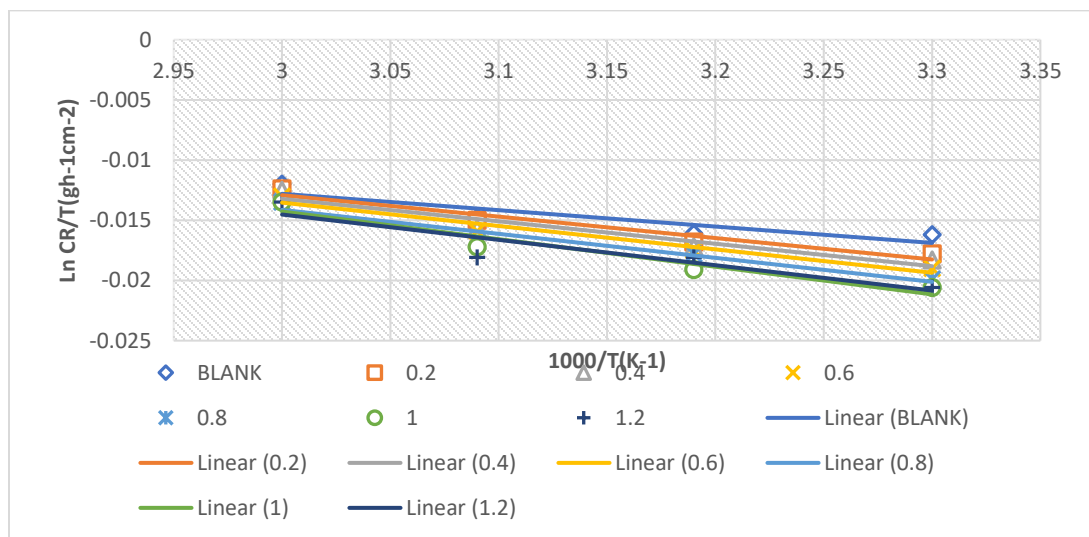
Fig.10: *Transition state plots for different concentrations of* TG Dye *and blank ..Relationship between ln CR/T and 1/T* for mild steel in 1 M HCl solution in different concentration of TG dye

Table 3: Thermodynamic parameters of various concentrations of TG Dye

CONCENTRATION (gL^{-1})	ACTIVATION ENERGY E$_a$ (KJ mol^{-1})	ENTALTY Enthalpy ΔH^o (KJ mol^{-1})	ENTROPY ΔS^o (J mol^{-1}K^{-1})
Blank	25.39	22.72	-190.71
0.2	35.50	32.40	-187.81
0.4	37.36	34.64	-187.32
0.6	39.37	37.12	-186.39
0.8	42.29	39.57	-185.66
1.0	46.01	43.23	-184.56
1.2	47.54	44.87	-184.07

Adsorption Isotherms

Langmuir adsorption isotherm

How Effect the dye extracted from Tectona grandis affects on metal corrosion in a 1M HCl solution was investigated. The amount of metal that corroded by weight loss at different dye concentrations was measured, based on these measurements, they how much of the metal surface the dye molecules covered (surface coverage) was calculated. A model called the Langmuir isotherm was then used to describes how the dye molecules arrange themselves on the metal surface. The equation for this model is provided below:

$$\left({C}/{\phi\theta} \right) = C + \frac{1}{K} \qquad\qquad 5....(7)$$

Where the "equilibrium constant" (K) reflects how strongly the dye molecules bind to the metal surface, and another value (C) represents the concentration of the dye in the solution.

The value of (C/θ) against the dye concentration (C). This plot was shown in Figure 5 11.

The resulting graph is a straight line, which is a good sign. It indicates that the dye molecules behave according to the Langmuir isotherm model. Additionally, a value close to 1 for both the slope and the linear regression coefficient (R^2) strengthens this conclusion.

The straight lines in Figure 5 11 were used to calculate the "adsorption constant" (K). This constant tells us how strongly the dye molecules stick to the metal surface.

A scientific equation $G°_{ads} = -2\cdot303RT$ log $(55\cdot5K_{ads})$, was used to relates this adsorption constant (K) to another value called "standard free energy of adsorption" ($\Delta G°_{ads}$). This free energy basically tells us how favorable the adsorption process is. A negative value indicates a spontaneous process, meaning the dye naturally binds to the metal. (Table 4) shows the calculated free energy values ($\Delta G°_{ads}$) for the dye. All the values are negative, which confirms the spontaneous adsorption. These free energy values are less negative than -40 kJ/mol. This suggests that the dye molecules likely bind to the metal surface through a process called "physisorption." This type of binding involves weaker physical attractions compared to stronger chemical bonds.[21].
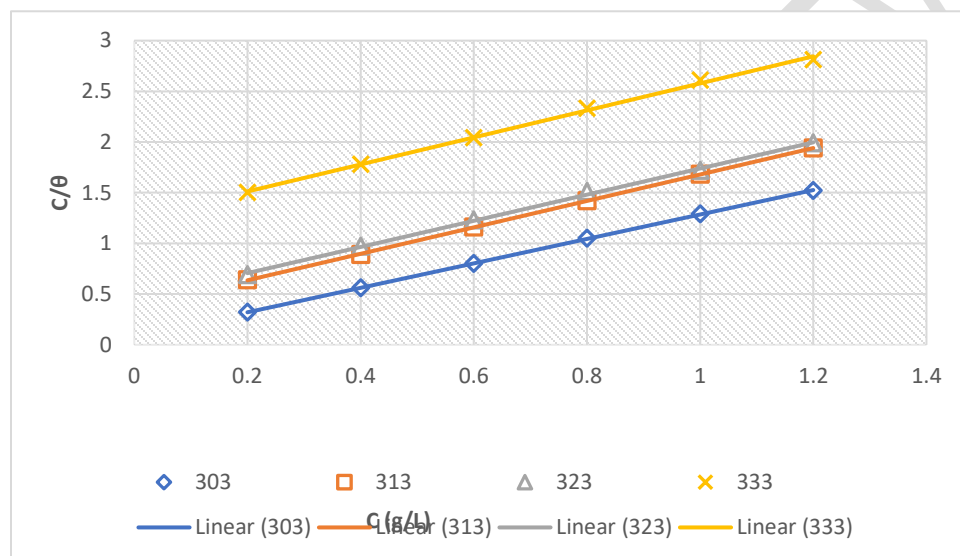
Fig.11: Langmuir adsorption isotherm of TG Dye   for mild steel in 1 M HCl solution in different concentration of TG dye

Table 4: Langmuir adsorption isotherm parameters

| Temperature(k)	R^2	$K_{ads.}$	Slope	$\Delta G°_{ads.}$
303	0.999	11.11	1.9	-16.18KJ
313	0.999	2.83	1.18	-13.16KJ
323	0.992	2.61	1.24	-13.36KJ
333	0.998	1.02	1.32	-11.17KJ

Freundlich Adsorption Isotherm

The Freundlich isotherm model, which may be expressed by equation 6, depicts the extent to which the inhibitor molecules cover the metal surface (surface coverage) at various concentrations of the inhibitor in the solution:

$$\text{Log}\theta = \text{LogK} + \frac{1}{n}\text{LogC}$$

6 ….(8)

We can also better grasp how readily the dye molecules adhere to the metal surface as shown by the Freundlich model. This model's computed value of "1/n" indicates the degree of adsorption ease. Easy adsorption is indicated by values between 0 and 1. As per reference [22], an adsorption value of precisely $1/n = 1$ indicates a moderate level of difficulty, while values exceeding 1 indicate a higher level of complexity. Table 5 shows that at all temperatures, the "Freundlich isotherm constant," also known as the adsorption constant, has values that are all less than 1. This suggests that the dye molecules readily adsorb on the surface of the metal. Furthermore, the values of the correlation coefficient (R^2) are extremely near to 1. This is an additional encouraging indication that the dye molecules are benefiting from the adsorption process.
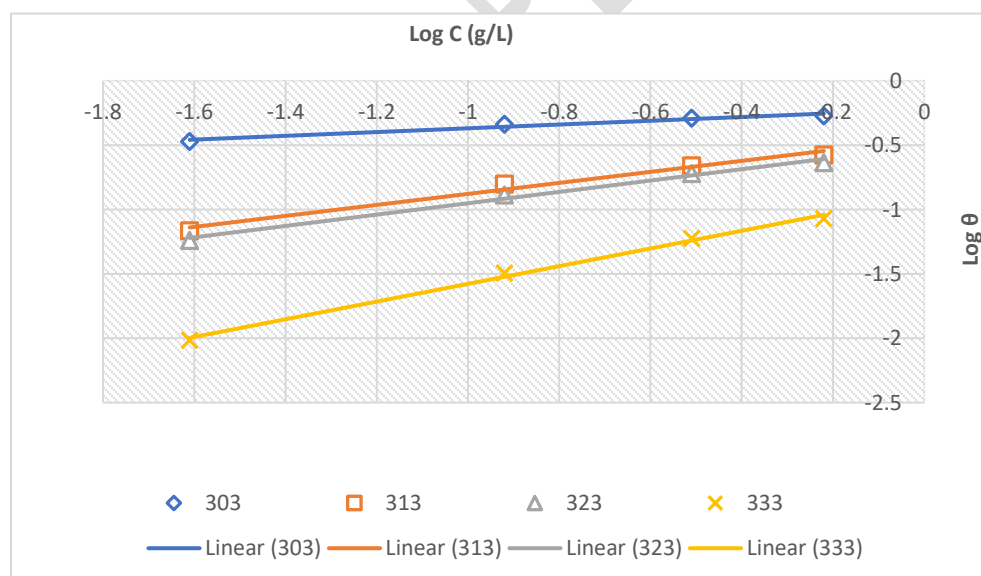
Fig.12: Freundlich adsorption isotherm of TG Dye   for mild steel in 1 M HCl solution in different concentration of TG dye

Table 5: Freundlich adsorption isotherm parameters

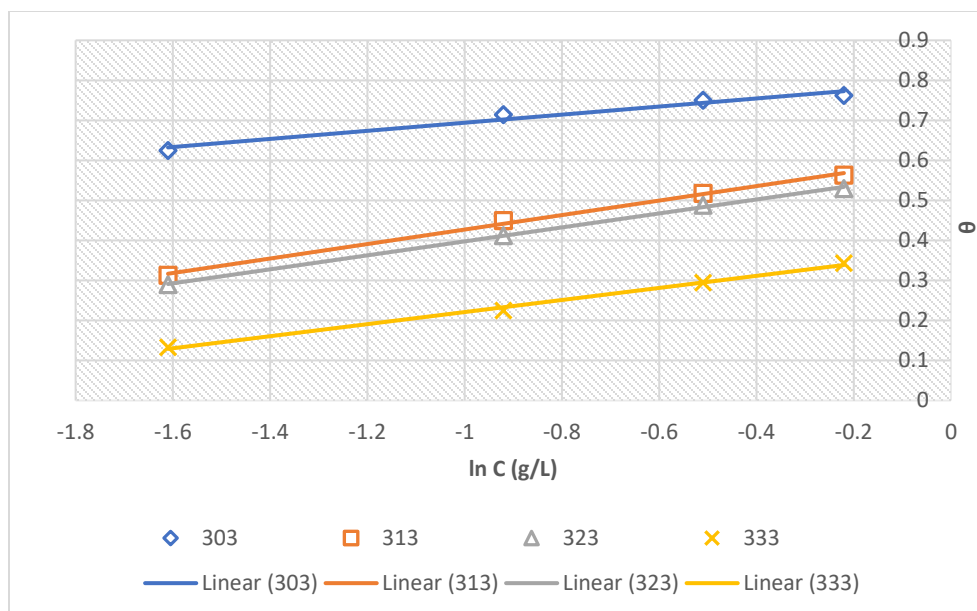| Temperature(k)	1/n	K_f	R^2
303	0.146	3.104	0.964
313	0.427	4.869	0.980
323	0.440	5.175	0.998
333	0.686	8.681	0.984

Temkin Adsorption Isotherm

The Temkin adsorption isotherm consider the effects of adsorbate /adsorbent interaction taking into assumption that the heat of adsorption of all molecules in a layer decrease linearly as the surface coverage increases [23]

Equation (8) (9) represents the linear equation of the Temkin adsorption isotherm model

$$\Theta\ \theta = RT/b\ \ln A + RT/b\ \ln C \qquad\qquad (7)....(9)$$

Where b is Temkin constant related to heat of adsorption in KJmol^{-1} and b Temkin equilibrium binding constant in Lg^{-1} [24]

The Temkin adsorption isotherm parameters were calculated and presented in figures 13 and tables 6 Table (6). The data obtained shows that all the value of b were positive and since this value is related to the heat of adsorption, then the adsorption of all the inhibitors onto the mild steel is endothermic which agree with the results from the thermodynamic evaluation studies.

Fig.13: Temkin adsorption isotherm <u>of TG Dye</u> for mild steel in 1 M HCl solution in <u>different concentration of TG dye</u>

Table 6: Temkin adsorption isotherm parameters

Temperature(k)	b(KJ/mol)	R^2
303	25.191	0.922
313	14.619	0.953
323	15.434	0.992
333	18.457	0.976

SEM analysis and EDX Analysis

The surface of mild steel (MS) before and after exposure to a strong acid 1M HCl solution was examined. Figure 14(a) shows a polished MS sample, representing the ideal smooth surface. Figure 14(b) shows the MS surface after 3 hours in the acid without any additives. The image reveals cracks caused by corrosion from the acid. To test the protective effect of the TG dye extract, MS sample was immersed in the same acid solution but with a tiny amount of the extract

(1.0 mg/L)(1.0 mg/l). Figure 14(c) shows the surface of this sample after 3 hours. Compared to Figure 14(b), there's much less damage, suggesting the extract significantly reduced corrosion. This significant difference is likely because the TG dye extract forms a strong layer on the metal surface when exposed to the acid solution. This layer acts as a barrier, protecting the metal from corrosion. Additional tests (EDX Composition) EDX analysis support this conclusion that the TG dye extract effectively inhibits corrosion in the presence of strong acid.

Element Number	Element Symbol	Element Name	Atomic Conc.	Weight Conc.
26	Fe	Iron	57.83	93.37
8	O	Oxygen	22.17	10.81
12	Mg	Magnesium	4.29	2.59
14	Si	Silicon	3.61	2.52
6	C	Carbon	1.71	0.51
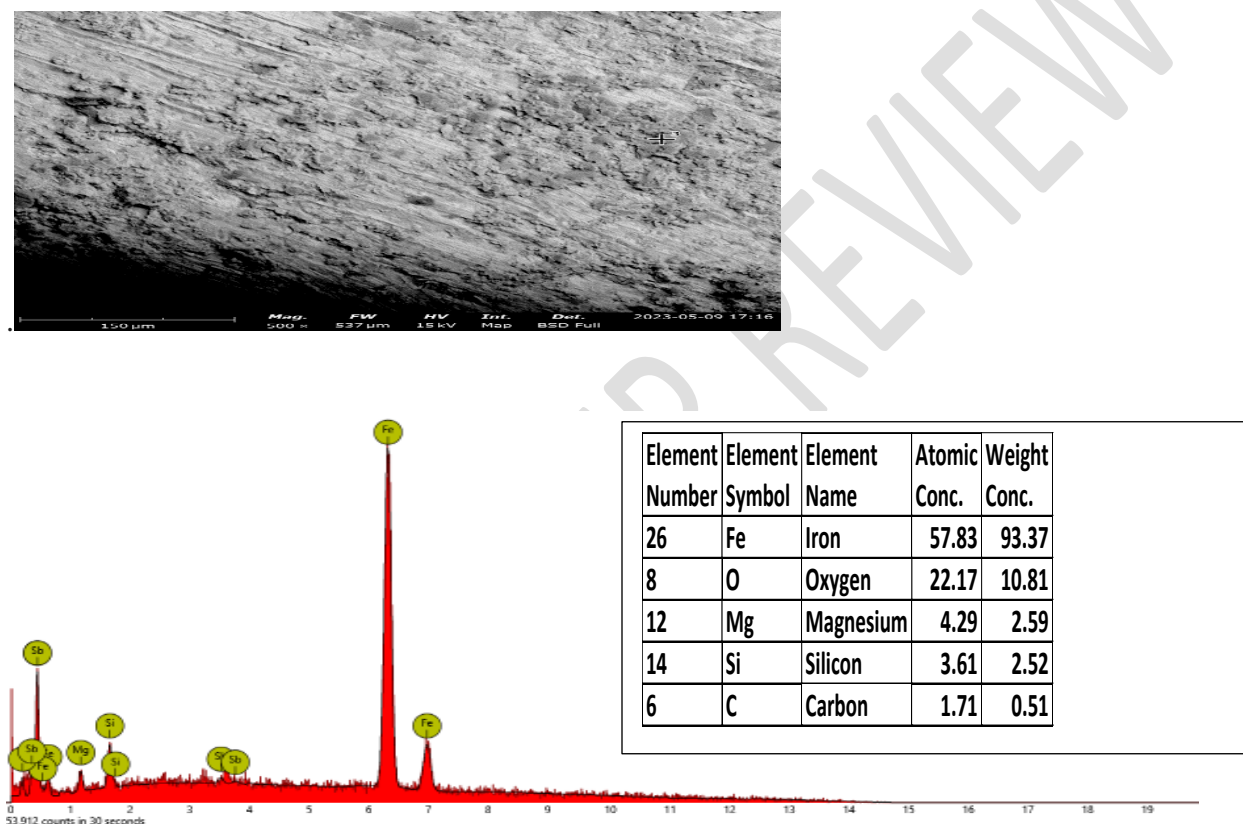
Fig 14(a): SEM image and EDX analysis of pristine mild steel

Element Number	Element Symbol	Element Name	Atomic Conc.	Weight Conc.
8	O	Oxygen	57.42	47.10
14	Si	Silicon	16.15	23.25
12	Mg	Magnesium	15.11	18.82
7	N	Nitrogen	7.96	5.72
6	C	Carbon	2.01	1.24
26	Fe	Iron	1.35	3.87
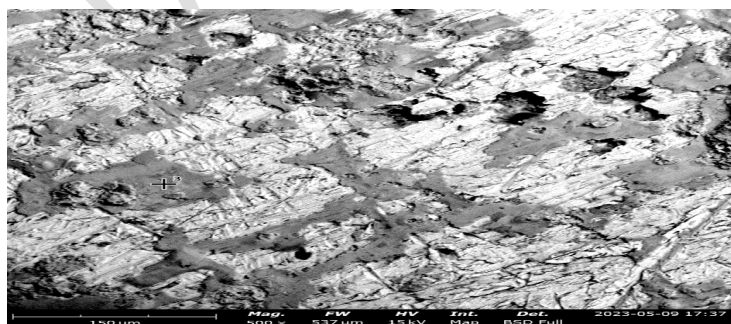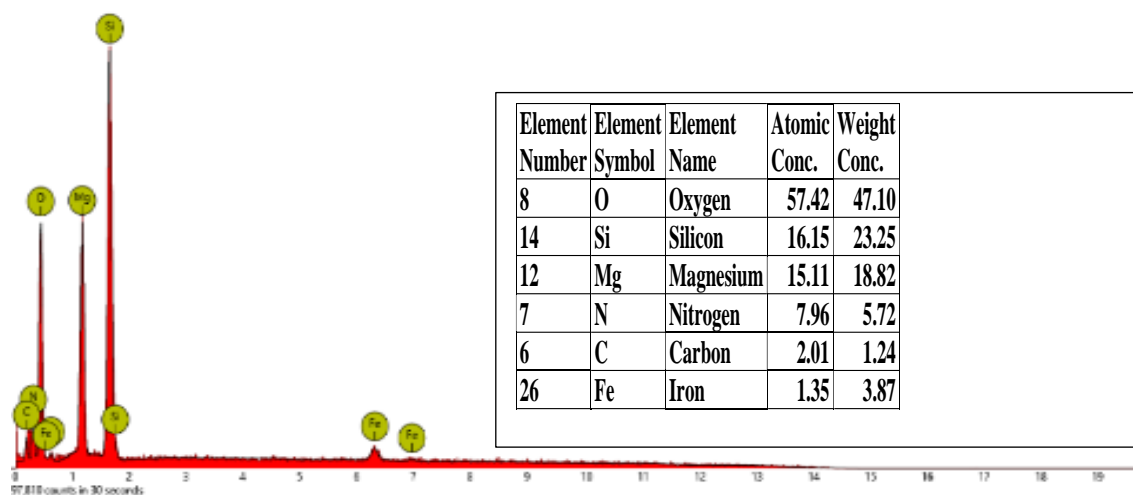
Fig14(b):SEM image and EDX analysis of mild steel after immersion in 1M HCl Blank solution

Element Number	Element Symbol	Element Name	Atomic Conc.	Weight Conc.
8	O	Oxygen	44.47	23.95
26	Fe	Iron	31.81	59.79
6	C	Carbon	9.67	3.91
12	Mg	Magnesium	7.38	6.04
14	Si	Silicon	6.67	6.31
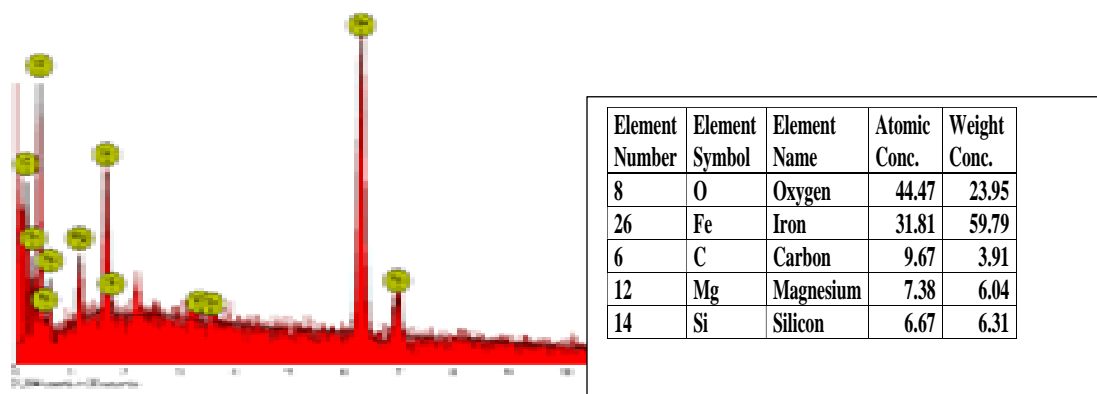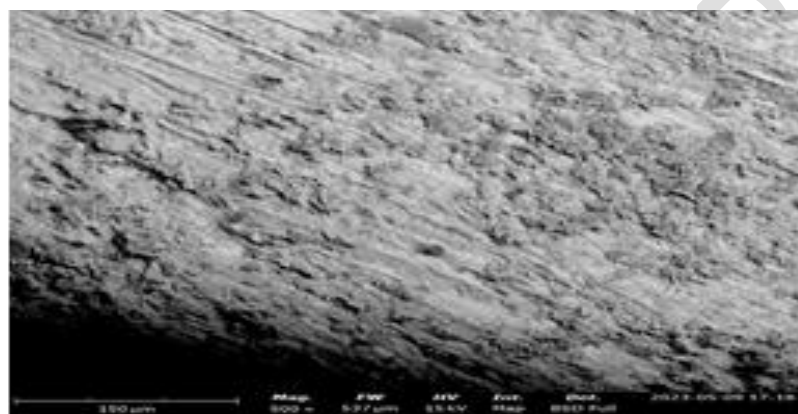
Fig14(c): SEM image and EDX analysis of Mild steel after immersion into TG Dye inhibitor solution

CONCLUSION

This study showed that increasing the concentration of the TG Dye extract improved its corrosion inhibition efficiency on mild steel. However, efficiency decreased as temperature rose. This temperature dependence is linked to the higher activation energy required for inhibited corrosion compared to uninhibited cases. Negative values of ΔH^o indicate an endothermic reaction, meaning the process absorbs heat. A negative ΔG^o_{ads} value suggests the inhibitor spontaneously adsorbs on the metal surface. The adsorption process follows obey Langmuir and Freundlich isotherms.

RECOMMENDATION

Based on the findings, the *Tectona grandis* dye can be used as eco-friendly inhibitors for mild steel in 1M HCl solution.

REFERENCES

1. Udhayakala, P., Jayanthi, A., Rajendiran, T.V., : Adsorption and Quantum Chemical Studies on the Inhibition Potentials of Some Formazan Derivatives. , *Der Pharma Chemica,* 2011 ,3, 528-539.

2. Okoronkwo, A. E., Olusegun, S.J., Olaniran, O.,; Acid extract of *Gliricidia sepium* leaves as green corrosion inhibitor for mild steel in HCl solutions, *African corrosion Journal.* , 2015, 1, 30- 35.

3. Akalezi C.O. , Oguzie E.E.,.; Evaluation of anticorrosion properties of chrysophy llum albdum leaves extract for mild steel protection in acidic media. , *International Journal of Industrial Chemistry*, 2016 ,7:81-92.

4. Peter, A. , Sharma, S.K. ; Use of *Azadirachta indica* as green corrosion inhibitor against mild steel in acidic medium., *International Journal of Corrosion Scale Inhibition*, 2017. , 6(2), 112-131.

5. Ashvin, G.G. , Rajaram ,S.S. ; Phyto chemical analysis of leaves of *Tectona grandis linn.* , *Int J Pharm Bio Sci*, 2014, 5,355 – 359

6. Sumithra, K. , Kavita , Y., Manivannan, R., Noyel ,V.S.; Electrochemical investigation of the corrosion inhibition mechanism of *Tectona grandis* leaf extract for SS304 stainless steel in hydrochloric acid, *Corros. Rev.*, 2017, 35, 111–121.

7. Ovili, A.O., Isaac, E.O., Ndor ,V.M. , ; Corrosion Control of Aluminium Alloys Using Teak Tree Leaf Extract , *Journal of Newviews in Engineering and Technology* (JNET), 2020,2,17-24

8. Karthikeyan ,S. , Abuthahir, S.S.S., Begum , A.S. , Rajendran ,S. , ; Inhibition of mild steel corrosion in 0.5 M sulfuric acid by an aqueous extract of leaves of *Tectona grandis L.* plant, *Int. J. Corros. Scale Inhib.,* 2021,10,1531–1546.

9. Trease G.E., Evans W.C., Phyto chemicals. In: Pharmacognosy. (15th edn), Saunders Publishers, London, 2002.

10. Khalid, S., Shahzad, A., Basharat, N., Abubakar, M., Anwar, P. , ; Phytochemical Screening and Analysis of Selected Medicinal Plants in Gujrat. , *J Phytochemistry Biochem* 2, 2018,108.

11. Olasehinde E.F., Agbaffa , B.E. , Adebayo M.A., Enis , ; J.,Corrosion protection of mild steel in acidic medium by titanium-based nanocomposite of *Chromolaena odorata* leaf extract, *Materials Chemistry and Physics* , 2022 ,281,1-10.

12. Miroslav S. , Susan L.B. , Daneel F. , Jan,, H.V.; Phytochemistry of Flavonoids and Molecules, 2010 , 15, 5196–5245

13. Naira N., , Karvekar, M.D. , ; Isolation of phenolic compounds from the methanolic extract of *Tectona grandis. , Research Journal of Pharmaceutical Biological and Chemical Sciences,* 2010, 1, 221-225

14. Agbaje L., Musibau A. A., Tesleem B. A., Taofeek A. Y., Akeem A., Iyabo C. O., Luqmon A., Sadiat E. A., Sunday A. O., Evariste B. G., and Lorika S. B., ; Biogenic synthesis of silver nanoparticles using a pod extract of *Cola nitida*: Antibacterial and antioxidant activities and application as a paint additive, *Journal of Taibah University for Science,* 2016.10, 551–562

15. Emeka, E.E. ,Ojiefoh, O.C., Aleruchi, C. , Hassan, L.A. , Christiana , O.M., Rebecca, M., Dare, E.O. and , Temitope, A.E., ; Evaluation of antibacterial activities of silver nanoparticles green-synthesized using pineapple leaf (*Ananas comosus*), *Micron, 2014* , 57, 1–5.

16 Shankar, S., Jaiswal, L., Aparna, R.S.L. & , Prasad, R.G.S.V.,; Synthesis , characterization, in vitro biocompatibility, and antimicrobial activity of gold, silver and gold silver alloy nanoparticles pre-pared from *Lansium domesticum* fruit peel extract, *Mater. Lett*., 2014,137 ,75–78

17. Sanatkumar B.S. , Nayak, Nityananda Shetty, A.,; Influence of 2-(4-chlorophenyl)- 2-oxoethyl benzoate on the hydrogen evolution and corrosion inhibition of 18 Ni 250 grade weld aged maraging steel in 1.0 M sulfuric acid medium, *Int. J. Hydrogen Energy*,(2012), 379431–9442

 18. Eddy, N. , Ebenso, O., ; Adsorption and inhibitive properties of ethanol extracts of *Musa saprentum* peel as a green corrosion inhibitor for mild steel in H_2SO_4, *African journal pure and Applied Chemistry*,2008, 6, 46- 54.

19. Okafor P.D., Osabor V.I., & Ebenso E.E.; Eco-friendly corrosion inhibitors: Inhibitive Action of Ethanol Extracts of *Garcinia Kola* for the Corrosion of Mild Steel in HNO_3 Solution *Pig Mort Resin Technol*, 2005, 36, 299–301.

20. Kathirvel, K., Thirumalairaj, B., Jaganathan, V. ; Quantum Chemical Studies on the Corrosion Inhibition of Mild Steel by Piperidin-4-One Derivatives in 1 M H_3PO_4. , *Open Journal of Metal*, 2014, 4, 73-85.

21. Mistry, B .M., Patel, N.S., Sahoo, S., Jauhari, S. ; Experimental and quantum chemical studies on corrosion inhibition performance of quinoline derivatives for MS in 1N HCl, *Bull. Mater. Sci.,2012,* 35(3), 459–469.

22. Ituen, E. , Akaranta ,O., James., A., ; Evaluation of performance of Corrosion Inhibitors using adsorption isotherm models: An overview , *Chemical Science International Journal*, 2017,18(1), 1-34.

23. Shahbeig, H., Bagheri, N., Ghorbanian, S.A., Hallajisani, A. and , Poorkarimi, S. A.; new adsorption isotherm model of aqueous solutions on granular activated carbon, *World Journal of Modelling and Simulation,*2013, 9(4), 243-254.

24. Ayawei, N., Ebelegi, A.N., Wankasi, D. , ; Modelling and Interpretation of Adsorption Isotherm, Journal of Chemistry, 2017,